NUMERICAL MODEL OF UOE STEEL PIPES: FORMING PROCESS AND STRUCTURAL BEHAVIOR

Javier Raffo, Rita G. Toscano, Luciano Mantovano and Eduardo N. Dvorkin

Center for Industrial Research (CINI), Tenaris, Dr. Jorge A. Simini 250, 2804 Campana, Argentina, jlraffo@tenaris.com, http://www.tenaris.com

Keywords: UOE, Pipelines, Collapse, Residual Stress.

Abstract. Deepwater pipelines are designed to withstand, without collapsing, the external pressure and bending imposed on them, either by the laying process or by the topology of the sea bottom. In previous publications CINI researchers have developed finite element models to predict collapse loads and collapse propagation loads.

Large diameter pipes for onshore and offshore applications are manufactured using the UOE process. The manufacturing process consists in the cold forming of heavy plates followed by welding and then by an expansion. First the plate is pressed along its edges, formed into a U-shape and then pressed into an O-shape between two semicircular dies. Afterwards the pipe is welded by SAW process and finally is expanded.

In this paper we develop a 2D finite element model to simulate the UOE process and the structural behavior of the formed pipes in external pressure collapse tests. Using the developed model we can analyze the effects of the process parameters in each forming step on the final geometry and structural properties of the pipe.

1 INTRODUCTION

The UOE process is composed by a cold forming stage, then the SAW welding and finally an expansion. During the forming stage the plate edges are bent into a circular shape using a press; afterwards the plate is formed in the "U" press followed by the forming in the "O" press. Then the formed plate is welded, using the SAW process, to produce a pipe. Finally this welded pipe is expanded with a mechanical expander. This manufacturing process introduces plastic deformations and residual stresses in the initial unstrained plate material.

A 2D finite element model is developed to describe the UOE process. The data that we use for the model input is obtained from CONFAB specifications (process and tooling).

The manufacture processes of a 12.75" OD 0.5" WT X60 and of a 18.0" OD 1.0" WT X60 UOE welded pipes are modeled.

A sensitivity analysis aimed at the investigation of the effects of the steel's strain hardening and of some process parameters on the pipes structural behavior is performed using the developed finite element model.

We compare the numerical results with the experimental ones obtained at C-FER Technologies (Edmonton, Alberta, Canada).

2 FINITE ELEMENT MODEL

For the numerical simulation of the UOE process, a finite element model using the Q1-P0 plane strain element in the ADINA general-purpose code (ADINA SYSTEM, K.J. Bathe, 1996) was developed. The numerical model was developed using a material and geometrical nonlinear formulation, taking into account large displacements/rotations but small strains (K.J. Bathe, 1996). Regarding the elasto-plastic material model, we use the von Mises associated plasticity model with a linear kinematic hardening.

During the collapse tests performed at C-FER the tensile / compressive hoop yield stresses were determined for fibers located close to the OD and ID respectively. Hence, we use as the yield stress of the unstrained material:

$$\sigma_y = \frac{1}{4} \cdot \left(\hat{\sigma}^+{}_y + \breve{\sigma}^+{}_y - \hat{\sigma}^-{}_y - \breve{\sigma}^-{}_y \right) \quad (1)$$

Where $\hat{\sigma}^+{}_y$ is the internal diameter sample, tensile test; $\hat{\sigma}^-{}_y$ the internal diameter sample, compressive test; $\breve{\sigma}^+{}_y$ the external diameter sample, tensile test and $\breve{\sigma}^-{}_y$ the external diameter sample, compressive test (see Figure1).

The forming tools are modeled as rigid bodies and we use a sliding nodes contact algorithm to simulate the contact between the tools and the plates (ADINA SYSTEM, K.J. Bathe, 1996). Symmetry conditions are considered for the model. The plate is modeled with 4 elements through the thickness and 100 elements along the width, for the 12.75" OD pipe, while for the 18" OD pipe the amount of elements along the length is 155 (see Figure 2). Since the objective of our model is to determine the effect of the forming process on the external collapse pressure of the pipes, we established the mesh to be used using the simple test reported in Figure 3.

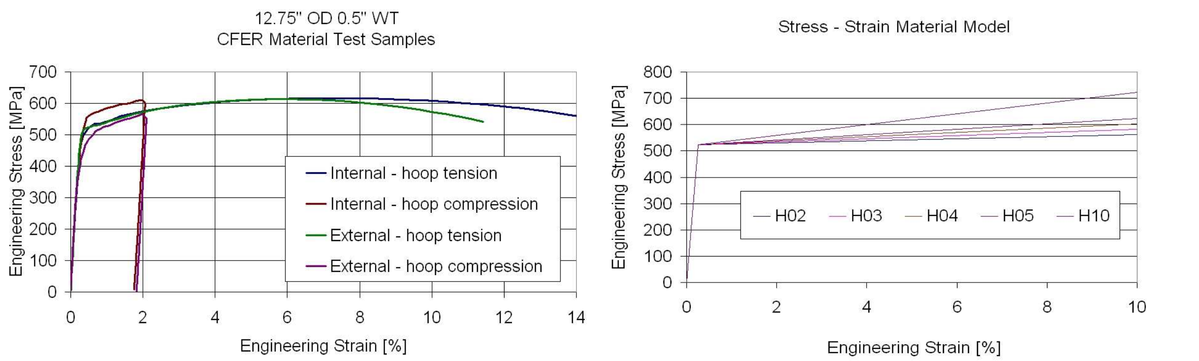

CFER hoop tests- 12.75” OD 0.5” WT X60 CONFAB-UOE pipe

Material model used in the numerical simulations

Figure 1. Material model.

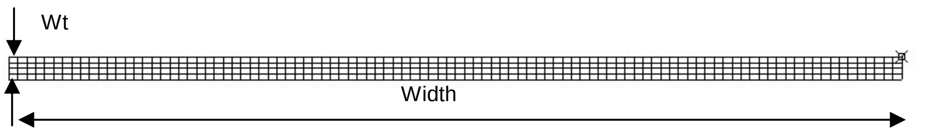

PIPE	Width [mm]	Wt [mm]
12.75” OD 0.5” WT X60	488.75	12.7
18” OD 1” WT X60	678.27	25.4

Figure 2. Plate dimensions.

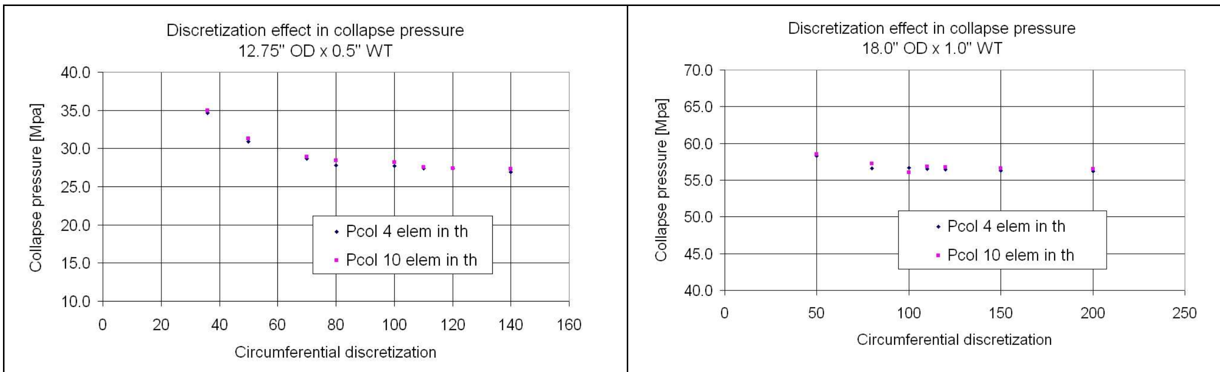

12.75” OD pipe

18” OD pipe

Figure 3. Effect of the finite element discretization on the external collapse pressure of a pipe

3 TOOLING

The first step of the manufacturing process is the edge press, during this process, the upper tool is fixed and the lower tool is moved in the Z direction. Figure 4 shows a representation of the real process vs. the FEM model.

Then the forming process continues with the “U” press, where the plate is formed into a U-shape (see Figure 5).

Afterwards, the forming process continues in the “O” press, where circumferential compression is applied to form an O-shape. To achieve this, two semi-cylindrical dies press the U-shape. Figure 6 compares the actual process with the FEM model.

At the point of maximum compression, the nodes of the pipe are fixed in the horizontal edge at the symmetrical axis. This is the way that the welding process is simulated.

Finally, a radial expansion is applied in order to obtain the final shape of the pipe. An internal mandrel with eight expansion segments is used for the OD 12.75” – WT 0.5” pipe and ten expansion segments for the OD 18” – WT 1” pipe. The segments move in radial direction, and expand so as to obtain the nominal perimeter when the load is released. Figure 7 compares the actual process with the FEM model.

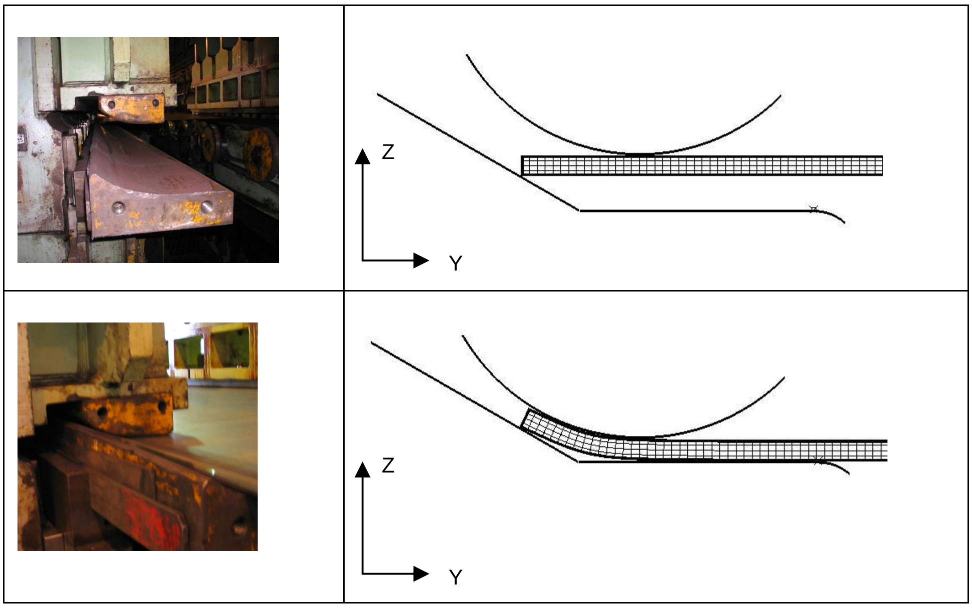

Figure 4. Edge press: real process and FEM model

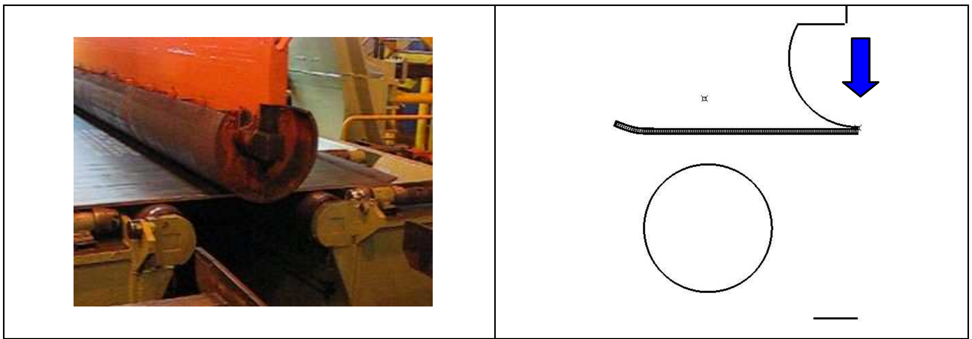

A) The pear goes down in the middle of the plate and pushes it up to contact the roller

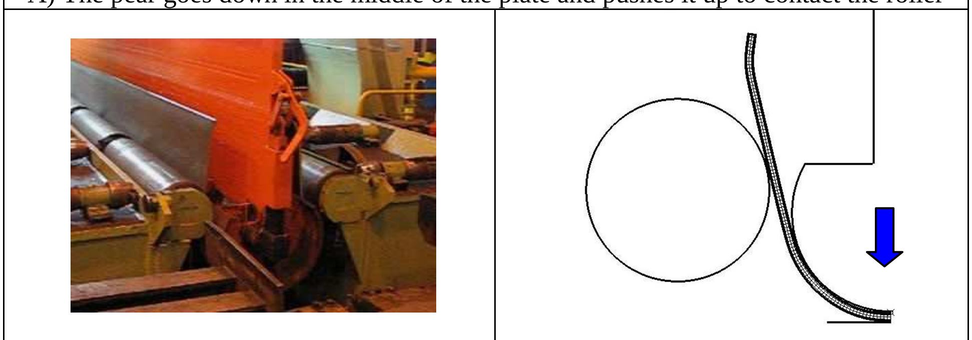

B) The pear continues going down up to a distance from the base that equals the plate thickness

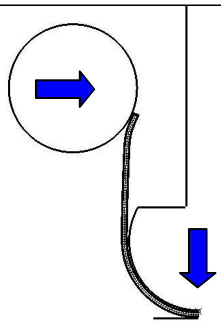

C) The pear and the base go down together, keeping a distance of one plate thickness between them. So the roller starts moving to the symmetry axis

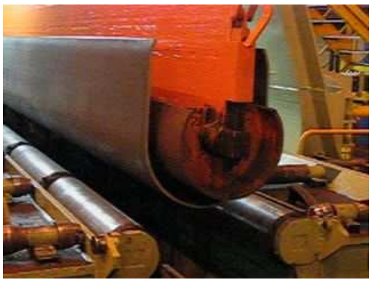

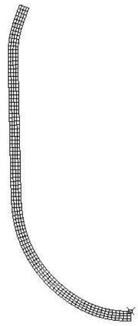

D) The pear moves to its limit and the load is released; then the plate is formed into an "U" shape

Figure 5. "U" Press: actual process and FEM model

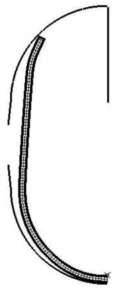

A) The press starts pressing

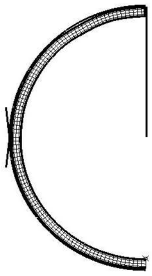

B) Maximum compression up to near 1.0% lower than the final diameter of the pipe

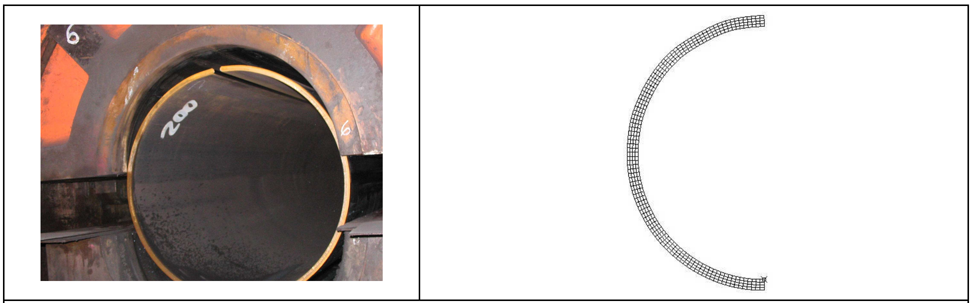

C) Load release and spring back of the "O" in the actual process and welded pipe obtained in the model

Figure 6. "O" press: actual process and FEM model

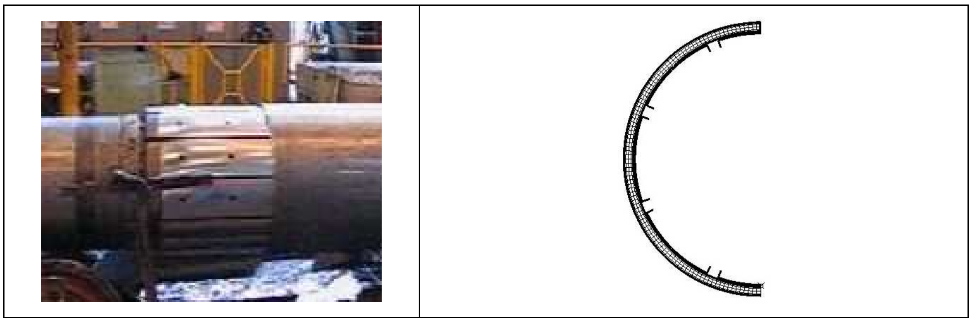

A) Expansion

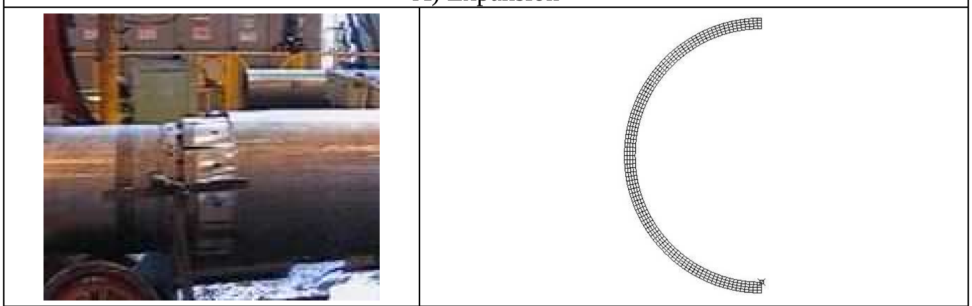

B) Release

Figure 7. Mechanical expansion after welding: actual process and FEM model

4 NUMERICAL RESULTS: GEOMETRY

4.1 Fourier Analysis of the Resulting OD Shapes.

An analysis of the OD shape obtained with the numerical simulation of the forming process is performed using Fourier decomposition, as described in Assanelli et al (2000). The position of the nodes on the outer surface is used as initial data.

$$r(\theta) = R_o + \sum_{j=1}^{N} \left[a_j \cos(j\theta) + b_j \sin(j\theta) \right] \tag{2}$$

Where Ro is the best-fit circle and the amplitude of mode j is:

$$A_j = \sqrt{(a_j)^2 + (b_j)^2} \tag{3}$$

being a_j and b_j the coefficients of Fourier decomposition.

Figure 8 shows the modal distribution for both pipes, when the model strain hardening is 0.5 % of the Young's modulus. It is interesting to observe the relative larger amplitude of the modes corresponding to the number of segments in the expander. The ovality is calculated with the following expression:

$$Ov = \frac{OOR}{Daverage}[\%] = \frac{D_{max} - D_{min}}{Daverage}[\%] \tag{4}$$

Figure 9 shows, for the different hardening values considered in the analyses, the ovalities after “O” and “E” processes, considering only mode 2 amplitude (OvM2) and considering all the modes (Ovx). The later represents the ovality value measured with an API ovalimeter.

Finally, Figure 10 shows the variation of the external radius along the circumference, after the expansion, for both pipes. For the first pipe the nominal radius values is 161.9 mm while for the second one is 228.6 mm. In the graphs position 0 corresponds to the welded region. The external radius obtained is slightly higher than the nominal one, but the average difference is low enough to consider that the UOE simulation met the manufacture requirement.

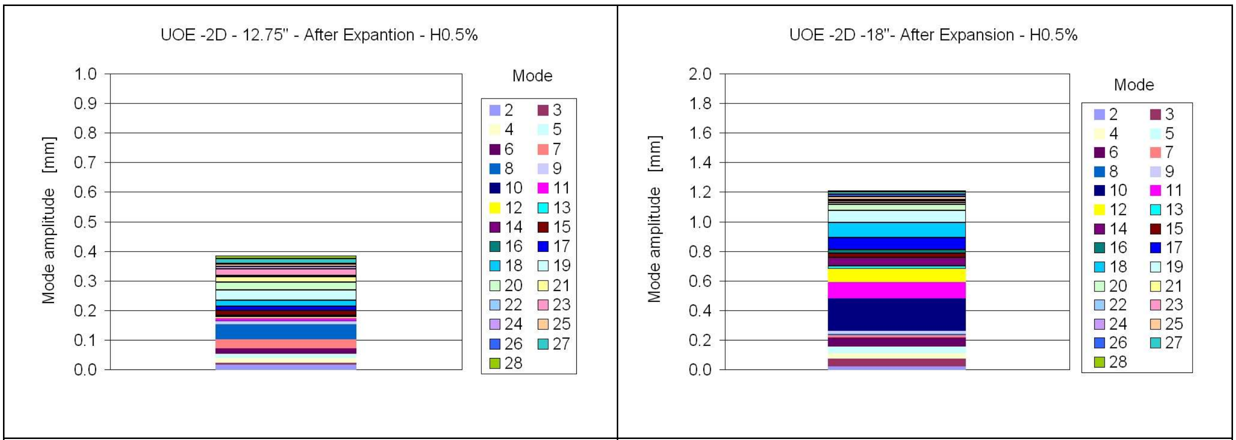

12.75” OD pipe	18” OD pipe

Figure 8. Modal analysis. Mode amplitude distribution after the expansion - Strain Hardening 0.5 %

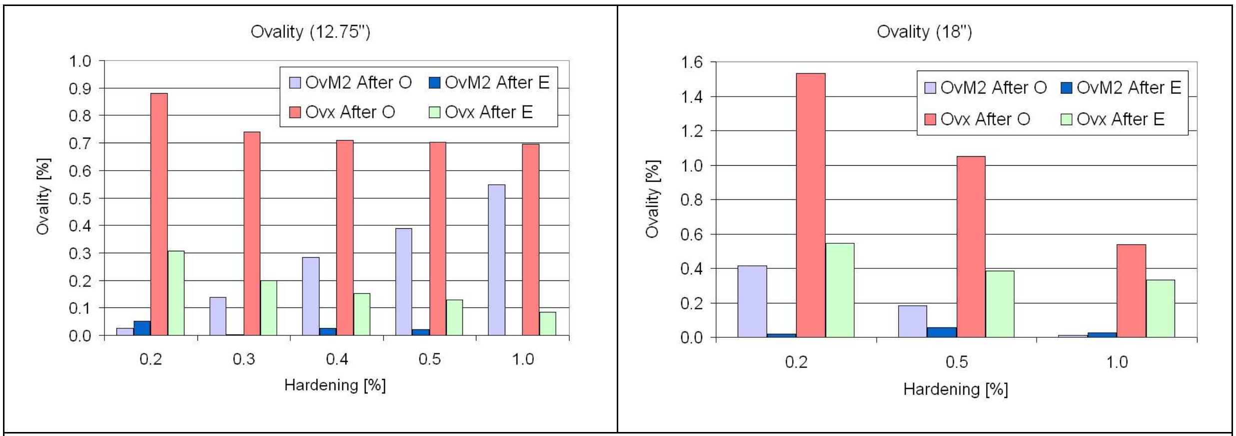

12.75” OD pipe	18” OD pipe

Figure 9. Ovality comparison for each hardening, considering mode 2 contribution only (OvM2) and ovality measured with ovalimeter (Ovx). After O pressing and after the expansion

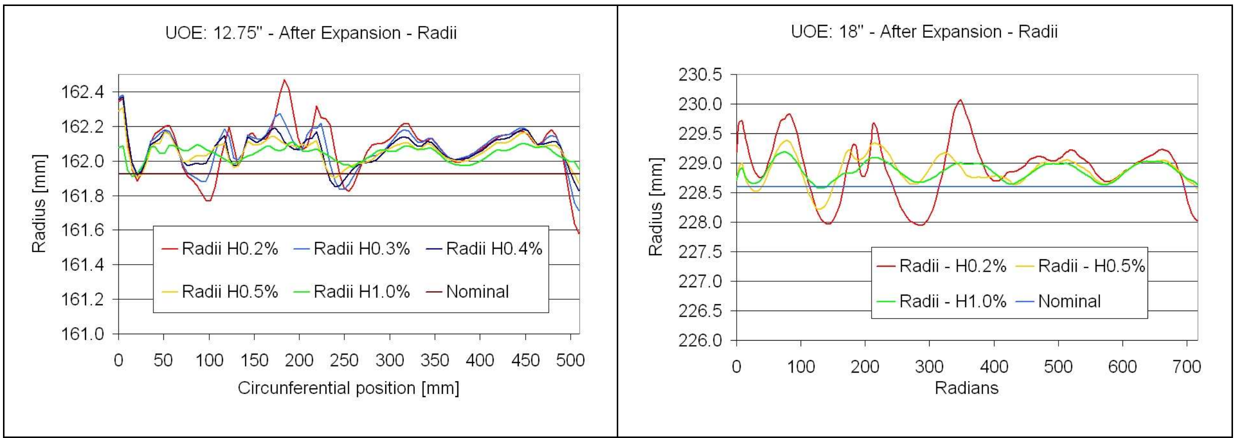

12.75” OD pipe	18” OD pipe

Figure10. External radius variation along circumference for each hardening after expansion

Summarizing we can observe,

- The ovality is much lower after the expansion than after the “O” process, and it diminishes as the hardening increases.
- As it was shown in Assanelli and Turconi (2001), the value of the ovality calculated taking into account only the second mode is quite different (lower) from the ovality measured with a standard API ovalimeter. The imperfection that controls the value of the collapse pressure is the second mode (Assanelli et al., 2000).
- After the “O” press, the variation of the ovality with the hardening is different for both pipes (different OD and different D/t ratio). We can justify this observation by taking into account that for the larger D/t ratios the spring back effect is larger.
- In the Fourier decomposition of the external surface, the modal distribution changes after expansion not only in amplitude but also in the relative importance among the modes.
- The modal distribution is different for both pipes.
- It can be observed that the external radius variation diminishes as the hardening modulus increases.

Therefore, it can be drawn that the imperfections of the final shape of the pipes (deviation from the perfect circular shape) depend on their dimensions (OD, D/t) as well as on the strain hardening modulus.

4.2 Strains

The geometry of the formed pipe and the mean circumferential deformation are calculated taking into account the final node locations. A manufacturing requirement is that the external perimeter at the end of the process must be the nominal perimeter; therefore, after the “O” press, it is necessary to apply an expansion high enough to meet this requirement. To calculate the mean circumferential compression and expansion strains the mid-surface perimeters are considered.

$$\varepsilon_C = -\frac{P_O - P_P}{P_P}[\%] \qquad \varepsilon_E = \frac{P_E - P_O}{P_O}[\%] \tag{5}$$

Where P_P is the initial plate length, P_O is the mid-surface perimeter after press O, and P_E is the mid-surface perimeter after the expansion. Figure 11 presents the strains values mentioned above. It can be observed that the average expansion strain is close to 1.0 % for the 12.75” OD pipe while it is close to 1.3 % for the second pipe, 18” OD 1” WT. Both, compression and expansion strains present some variation with the strain hardening modulus, finding the lowest values for the highest hardening value.

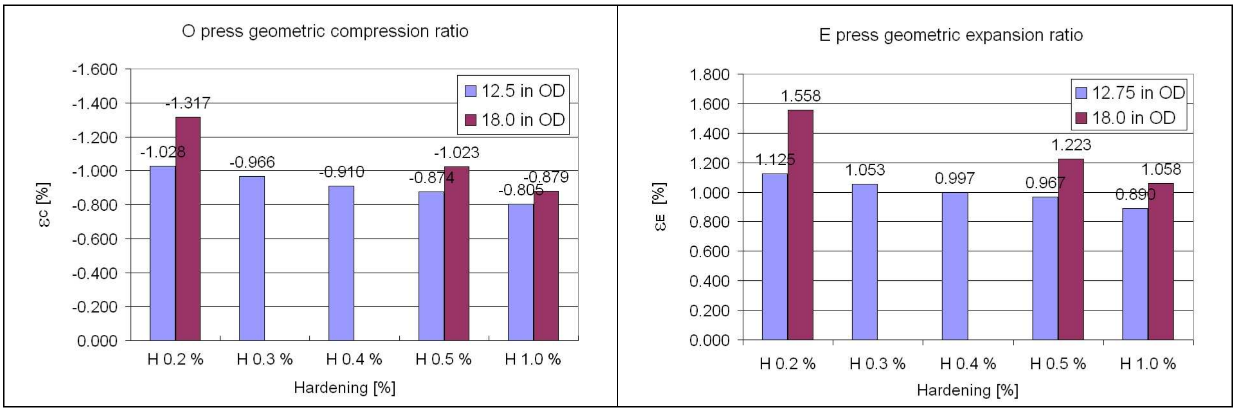

Figure 11. Mean mid-surface circumferential strain ε [%]

The thickness variations of the pipe after the UOE process for each hardening are described in Figure 12, where it can be observed that the thickness circumferential distribution is more uniform when the hardening value increases. Figure 13 shows the evolution of the thickness all along the UOE process for 0.5 % of hardening modulus. It is observed that the thickness circumferential distribution becomes more uniform after the expansion process. Therefore, the compression and expansion strains necessary to meet the process requirements, such as the nominal perimeter and nominal thickness, depend on pipe dimensions and on the material properties, such as the strain hardening.

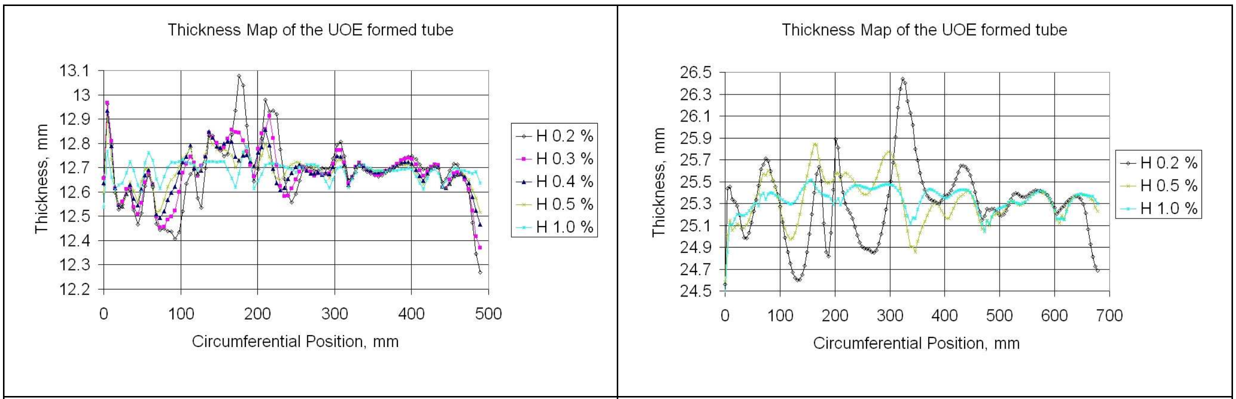

12.75” OD pipe	18” OD pipe

Figure 12. Thickness circumferential distribution at the end of the UOE process for all analyzed hardenings

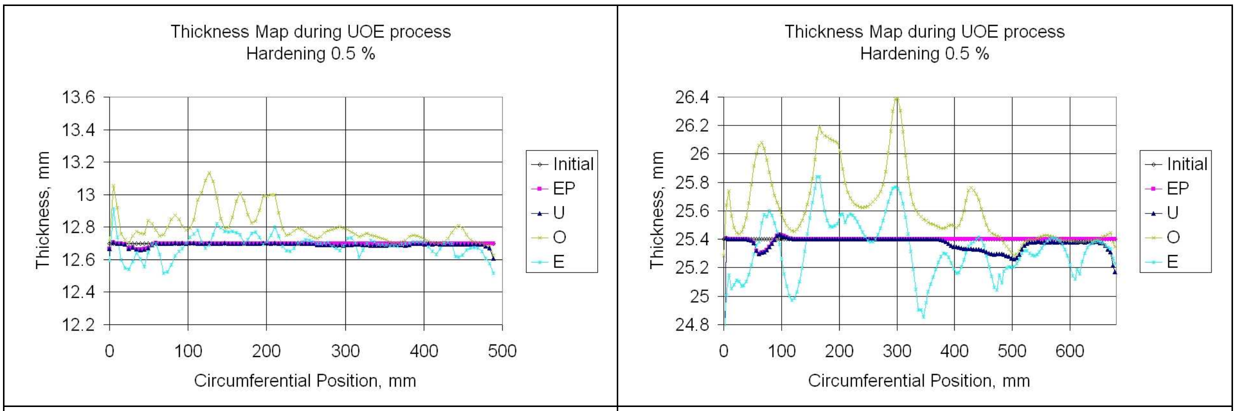

12.75” OD pipe	18” OD pipe

Figure 13. Thickness map during the forming process of the tube - Strain Hardening 0.5 %

5 NUMERICAL RESULTS: RESIDUAL STRESSES AND PLASTIC STRAINS

5.1 Residual stresses.

A slit ring test (Assanelli et al., 2000) is simulated after the forming process simulation to determine the residual stresses. It is done releasing the horizontal displacements of the nodes in the symmetrical edge fixed at the point of maximum compression during the “O” process. The measured openings are post-processed using the formula:

$$\frac{(D_c - D_E)\cdot t\cdot E}{(D_E - t)^2\cdot\left(1-\upsilon^2\right)} \qquad (6)$$

Where: D_E is the average outside diameter before the cut (the one obtained after the expansion); D_C is the average outside diameter after the cut; t is the average thickness of the sample; ν Poisson ratio and E, Young’s modulus. The results of this analysis are listed in Table 1. These results show that the residual stresses increase with strain hardening value and decrease when D/t ratio increase.

Strain hardening	12.75” OD D/t = 25.5 [MPa]	18” OD D/t = 18 [MPa]
0.2 %	9.20	7.37
0.3 %	21.7	-
0.4 %	33.0	-
0.5 %	44.3	59.07
1.0 %	96.4	140.8

Table 1. Simulated residual stresses

5.2 Stress – strain distributions.

Hoop stresses and strains after the expansion for each hardening in the outer surface are shown in Figure 14. Figure 15 shows the behavior of the hoop stress and strain during the forming process in the outer surface for 0.5 % hardening modulus. It can be observed that hoop strains are higher for 18” OD 1” in WT pipe than for 12.75” OD 0.5” WT, and the same happens with the hoop stresses, in accordance with the results presented above. Stresses as well as strains present a variation along the circumference (0 corresponds to the welded area); the strain variation is more notorious between 0° and 90° from the weld and is more uniform for higher strain hardening. It is clearly seen in the strains distribution that for the smaller hardening modulus there are important strain localizations during the forming process.

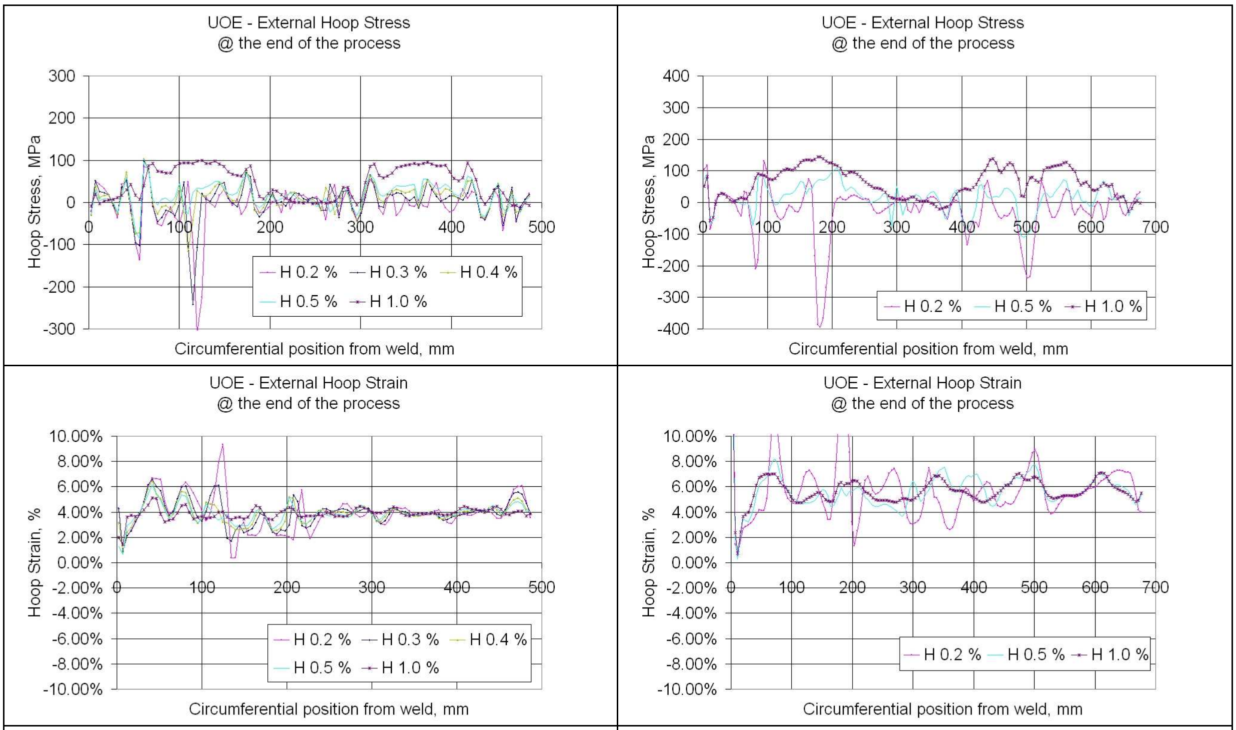

12.75” OD pipe	18” OD pipe

Figure 14. Hoop stresses and strains at the end of the process for all the hardenings analyzed, at outer surface of the pipe

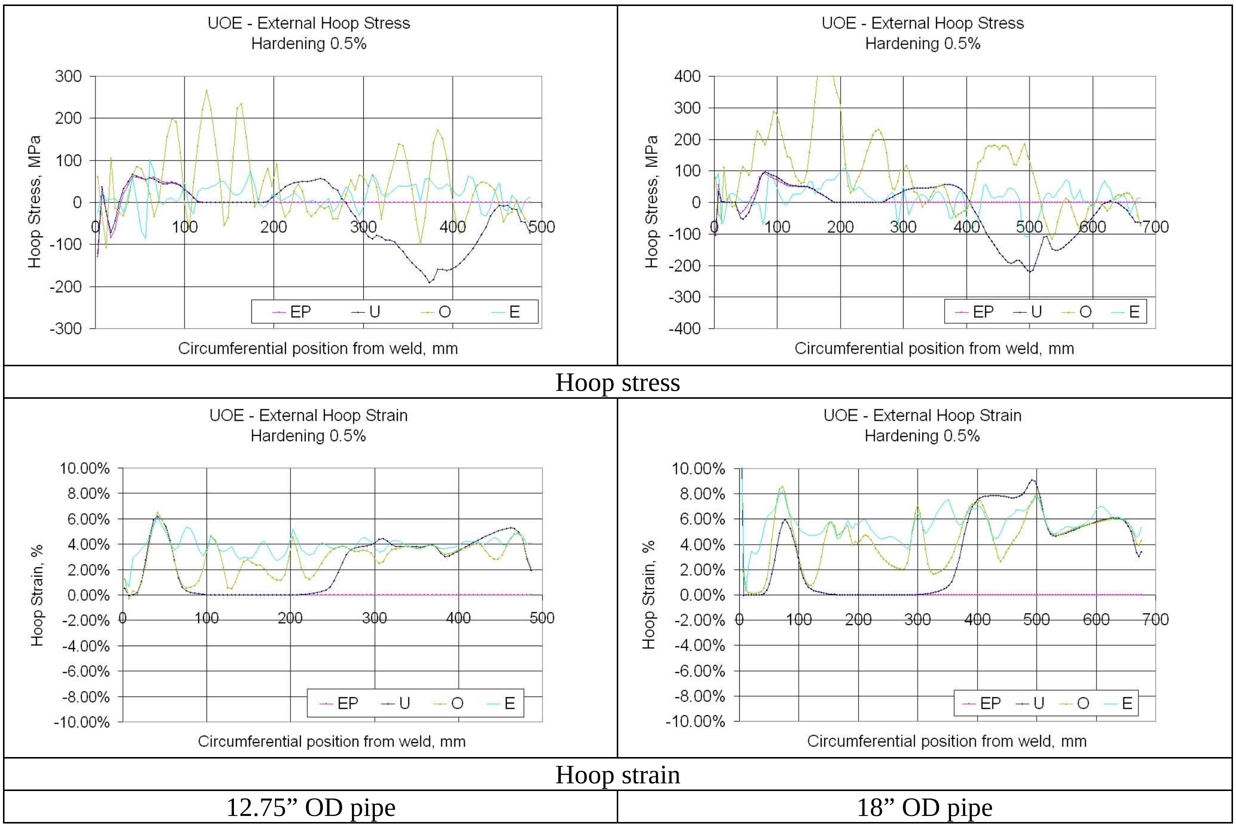

Figure 15. Hoop results at the end of each process for 0.5 % hardening modulus, at outer surface of the pipe

Figure 16 shows the accumulated effective plastic strain maps for both, the 12.75” OD pipe and the 18” OD pipe; these results correspond to strain hardening 0.5% at the end of the forming process. The Hoop Stress vs. Hoop strain curve of the entire process was obtained from the 0.5% hardening models. It was performed at 180° from the weld, at the integration points in the outer surface of the plate, see Figure 17.

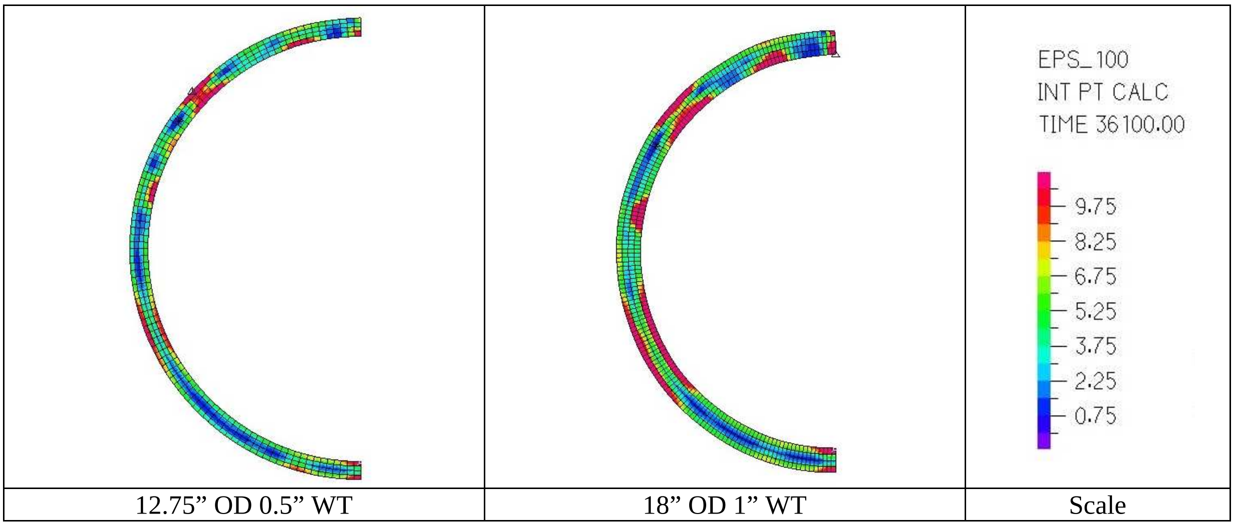

Figure 16. - Accumulated effective plastic strains [%] of the model at the end of the UOE forming process. Hardening: 0.5 %

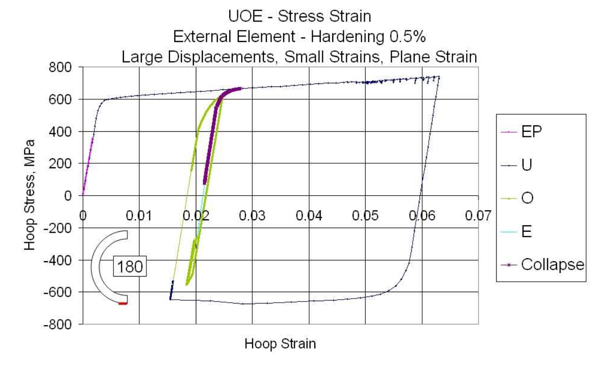	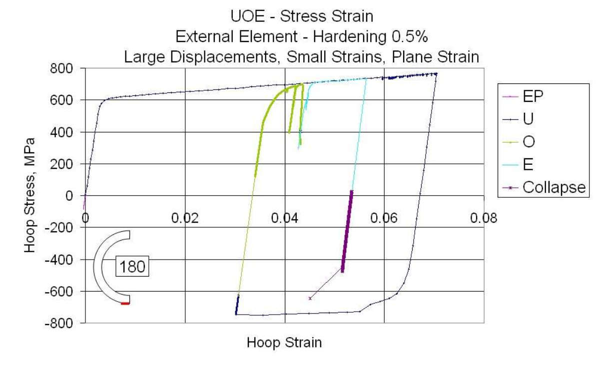
12.75” OD pipe	18” OD pipe

Figure 17. Hoop stress-strain curve during the process at 180° from the weld in the outer surface of the tube. Strain Hardening 0.5 %

5.3 Collapse.

After simulating the forming of the pipes we continue with the simulation of their behavior under external pressure, to determine the external collapse pressure. The external collapse pressure values are compared with those obtained from pipes with same geometry but without any residual deformation or residual stresses; that comparison is aimed to evaluate the degradation of the external collapse pressure induced by the UOE process. Table 2 and Table 3 summarize the results of that analysis.

Hardening	A) Collapse after UOE process [MPa]	B) Collapse with same geometry but virgin material [MPa]	Difference [%]
0.2 %	28.147	29.492	-4.56
0.3 %	27.819	29.010	-4.11
0.4 %	28.715	28.514	≅0
0.5 %	28.399	28.269	≅0
1.0 %	29.315	29.012	≅0

Table 2 – Collapse pressure. 12.75” OD x 0.5” WT

Hardening	A) Collapse after UOE process [MPa]	B) Collapse with same geometry but virgin material [MPa]	Difference [%]
0.2 %	49.249	54.560	-9.73
0.5 %	53.665	56.937	-5.75
1.0 %	54.826	56.842	-3.55

Table 3 – Collapse pressure. 18” OD x 1” WT

For the first pipe, with D/t ratio 25.5, it can be observed that UOE process degrades the collapse pressure of UOE pipe only for the two lowest strain hardening values. For the second pipe, with D/t ratio 18, this effect can be observed for the three cases analyzed, being lowest the effect of the highest hardening value.

To understand the above results we should take into account the following points:

- For the largest D/t ratio the plasticity has less effect on the collapse pressure; hence the deterioration induced by residual stresses and Bauschinger effect is low and the deterioration is mostly induced by the geometry imperfections derived from the strain localizations during the forming process, which are smaller for larger hardening modulus.
- For the lowest D/t ratio the residual stresses and Bauschinger effect grow with the hardening, and this tends to deteriorate the external collapse pressure but the OD shape is also smoother when the hardening increases and this is beneficial for the external collapse pressure.

6 INFLUENCE OF THE COMPRESSION RATIO

An analysis of the compression ratio was performed to deduce the compression ratio used when the 12.75” OD 0.5” WT pipe was manufactured. The variables analyzed to perform this reverse engineering problem are: the second mode from Fourier analysis, collapse pressure and residual stresses. These three variables are compared with the experimental values obtained at CFER (collapse pressure and residual stresses) and CINI (second mode) from two samples. Figure 18 shows the distribution of the second mode all along the pipe and the two samples taken from this pipe, and it compares the measured variables with the ones obtained from the numerical model.

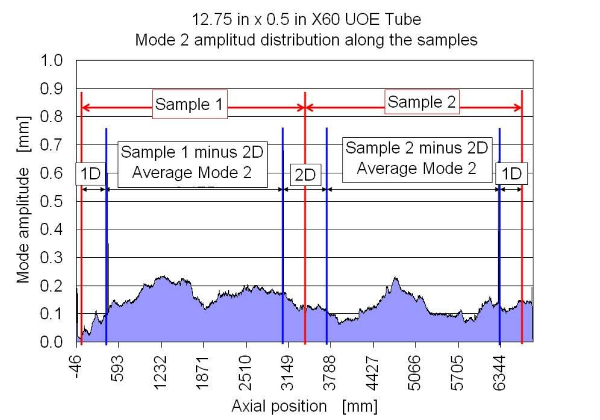

Second mode distribution along the two samples taken from the 12.75" OD 0.5" WT pipe

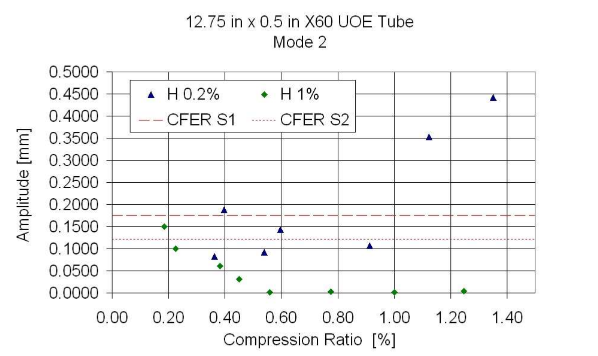

Mode 2 comparison of the samples and the obtained with the numerical model with different compression ratios

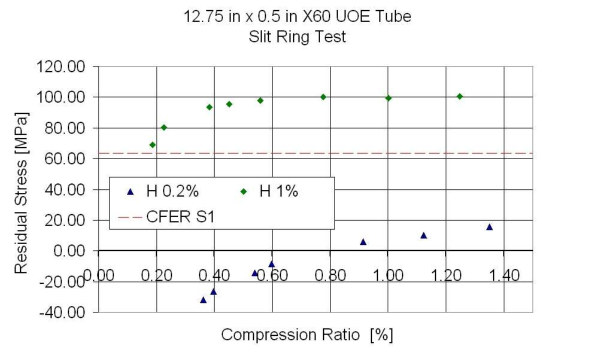

Residual stress comparison of the sample and the obtained with the numerical model with different compression ratios

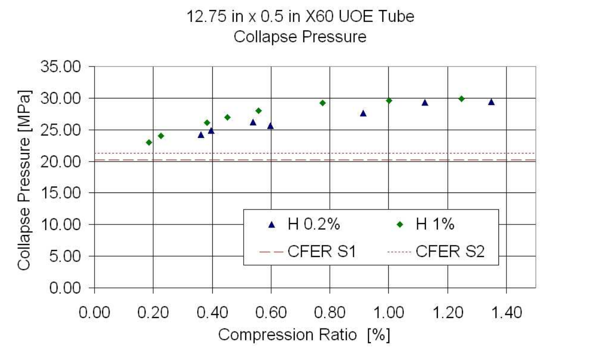

Collapse pressure comparison of the samples and the obtained with the numerical model with different compression ratios

Figure 18. Numerical vs. experimental results.

From Figure 18 it can be inferred that the compression ratio used during the forming process is near 0.2 % and this value is close to that usually used in CONFAB plant.

7 CONCLUSIONS

The FEM simulation of the UOE forming process and of the a posteriori external pressure test provided the following information:

Pipes geometry

- The imperfections in the final shape of the pipes (deviation from the perfect circular shape) depend on their dimensions (OD, D/t) as well as on the strain hardening modulus.
- The compression and expansion strains necessary to meet the process requirements, such as the nominal external diameter and nominal thickness, depend on pipe dimensions and on the material properties.
- It is clearly seen in the strains distribution that for the smaller hardening modulus there are important strain localizations during the forming process. In this cases therefore, the UOE process produces a more uneven geometry.

Residual stresses

- Residual stresses are higher for the lower D/t ratio pipes and increase with strain hardening value and compression ratio.

Collapse resistance

- We analyzed two pipes with D/t= 25.5 and 18. For both of them the deterioration in the collapse pressure was less than 5% and 10% respectively; numbers much smaller than the ones usually reported in the literature (Kyriakides et al. 2006, Fryer et al. 2004). This is because the compression ratio used in this work for the "O" press is much higher than the one reported in the above mentioned references.
- The deterioration of the collapse pressure induced by residual stresses and Bauschinger effect increases for lower D/t, while the deterioration for larger D/t is mostly induced by geometry imperfections.
- The influence of the strain hardening on the collapse pressure is low.

Compression ratio

- The collapse pressure and the residual stresses diminish for the lower values of the compression ratio, while the second mode increases.

8 REFERENCES

The ADINA SYSTEM, ADINA R&D, Watertown, MA, U.S.A.

K.J. Bathe, *Finite Element Procedures*, Prentice Hall, NJ, 1996.

A.P. Assanelli, R.G. Toscano, D.H. Johnson and E.N. Dvorkin, "Experimental/ numerical analysis of the collapse behavior of steel pipes", *Eng. Computations*, 17, pp.459-486, 2000.

A.P. Assanelli and G. López Turconi, "Effect of measurement procedures on estimating geometrical parameters of pipes", *2001 Offshore Technology Conference*, Paper OTC 13051, Houston, Texas, 2001.

K.J. Bathe and E.N. Dvorkin, "On the automatic solution of nonlinear finite element equations", *Computers & Structures*, 17, pp. 871-879, 1983.

Kyriakides S, Herynk M D, Yun H. Optimization of UOE pipe manufacturing process for improved collapse performance under external pressure. In: *Proceedings of International Pipeline Conference*, September 25-29, 2006, Calgary, Alberta, Canada.

Fryer M, Tait P, Kyriakides S, Timms C, DeGeer D. The prediction and enhancement of UOE-DSAW collapse resistance for deepwater pipelines. In: *Proceedings of the fifth biennial International Pipeline Conference,* October 4–8, 2004, Calgary, Alberta, Canada, vol. 3, p. 1961–6.